Electronic Supplementary Information (ESI)

Reformation of conjugated polymer chains toward maximum effective conjugation lengths by quasi-swelling and recrystallization approach

Horng-Long Cheng,*[a] Jr-Wei Lin,[a] Fu-Chiao Wu,[a] Wei-Ruei She,[a] Wei-Yang Chou,[a] Wei-Ju Shih[b] and Hwo-Shuenn Sheu[a,b]

[a] *Institute of Electro-Optical Science and Engineering, Center for Micro/Nano Science and Technology, and Advanced Optoelectronic Technology Center, National Cheng Kung University, Tainan 701, Taiwan, R.O.C.*

[b] *National Synchrotron Radiation Research Center, Hsinchu 30076, Taiwan, R.O.C.*

E-mail: shlcheng@mail.ncku.edu.tw

Content

1. Experimental details

Preparation of the P3HT Films*:* The P3HT films with a typical thickness (*t*) of ca. 60 nm were spin-coated from 0.34 wt% TCB and as the "initial film". Then, the films were baked at 120 ℃ for 2 h and as the "dry film". A PVDF buffer layer (*t* of ca. 20 nm) was spin-coated from 1 wt% DMF solution and heated at 150 ℃ for 1 h. The cPVP layer (*t* of ca. 950 nm) was spin-coated from a blend of 8 wt% PVP (M_w of 22,000 g/mol) and 4 wt% poly(melamine-co-formaldehyde) (M_w of 511 g/mol) in n-butanol solution and heated at 175 ℃ for 1 h. For comparison, an extra LiF layer (*t* of ca. 5 nm) between P3HT and PVDF layers was thermally evaporated under a pressure of 2×10^{-5} torr. All the chemical reagents were obtained commercially from Aldrich Chemical Co. and used as received. To study the effect of annealing on the P3HT films, the dry film was further annealed at 150 ℃ for 24 hours or 175 ℃ for 1 hour and as the "post-annealed film".

Characterization. The film thickness was determined by using an Alpha-step profilometer (Tencor Instruments, Alpha-step IQ). The absorption spectra were produced by a GBC Cintra 202 spectrometer with a scan rate of 1000 nm/min. At least three absorption spectra were recorded on each sample. MicroRaman spectra of the P3HT films, produced by lattice phonons, were obtained using a Jobin Yvon LabRam HR spectrometer. A 532 nm solid state laser served as the excitation light source and were kept below 0.5 mW to prevent thermal damage of theP3HT film. The spatial resolution of the beam spot was around 1 μm, obtained using a 100× objective microscope lens. The spectrometer resolutions are within 0.4 cm^{-1}. Every Raman spectrum was taken an average of ten spectrums and at least three spectra were measured for each sample. The GIXRD of thin film samples were performed at the BL17A1 beamline of the NSRRC. The ring of NSRRC was operated at energy 1.5 GeV with a typical current 300 mA. The wavelength of the incident X-rays was 1.3323 Å (9.3 keV), delivered from the wiggler magnet and a Si(111) triangular crystal monochromator. Two pairs of slits and one collimator were set up inside the experimental hutch to provide a collimated beam with dimensions of typical 1.0 mm0.5 mm (H x V) at the sample position. The grazing incident geometry was applied to measure the film samples. The grazing angle was large enough to probe the interior of the films and meantime small enough to increase the X-ray path length within the films by orders of magnitude. For an incident angle ~0.3, X-ray path length within a several thousand Angstroms thick film was several hundred microns. This significantly enhances the X-ray scattering intensity from the thin films. The

diffraction pattern was recorded with a Mar345 imaging plate detector approximately 300 mm from the sample and typical exposure duration 5 min. The pixel size of Mar345 was 100 μm. The one-dimensional powder diffraction profile was converted with program FIT2D and cake-type integration. The diffraction angles were calibrated according to Bragg positions of Ag-Benhenate and Si powder (NBS640b) standards.

Scheme S1. Simplified Scheme Illustrating the P3HT Structural Transformation Induced by Various Different Processes[a]

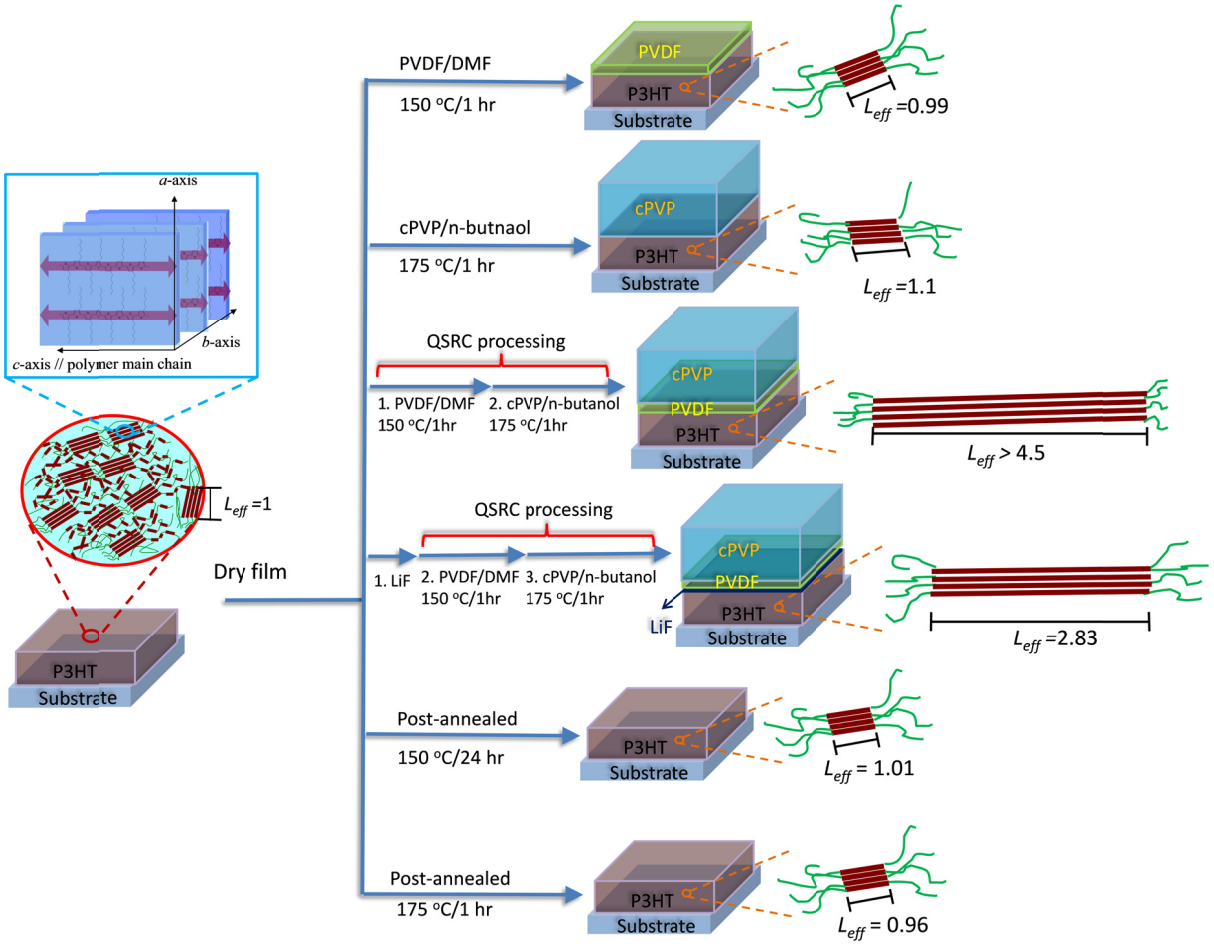

[a] The relative values of L_{eff} were taken from Table 1. The long conjugated and distorted segments are shown using heavy (brown color) and thin (green color) lines, respectively.

2. Supplementary absorption spectra and theoretical fitting procedure

According to recent theoretical predictions,[4] the absorption from crystalline regions and the magnitude of the exciton bandwidth (*W*) of P3HT can be estimated by fitting the absorption spectrum through a modified Frank-Condon analysis:[9]

$$A \propto \sum_{m=0}\left(\frac{e^{-S}S^{m}}{m!}\right)\left(1-\frac{We^{-S}}{2E_{P}}G_{m}\right)^{2}\Gamma\left(\hbar\omega-E_{0-0}-mE_{P}\right) \qquad \text{(S1)}$$

where *A* is the relative absorption intensity of the individual bands, *m* is the vibrational level, *S* is the Huang-Rhys factor, E_P is the energy of the main vibrational mode, G_m is equal to $\Sigma_{n(\neq m)}S^n/n!(n\text{-}m)$ (*n* is the vibrational quantum number), Γ is assumed as a Gaussian function, ω is the vibrational frequency, and $E_{0\text{-}0}$ is the energy of the 0-0 electronic transition. During the curve-fitting procedure, *S* is assumed to be 1 and a refractive index ratio of 0.97 between the A_0 and A_1 bands was used.[9] The simulation results are shown in Fig. 1B and Fig. S1.

To further confirm the importance of the buffer layer on the QSRC processing, we made other polymer insulators to use in a buffer layer upon the P3HT films to replace the role of PVDF/DMF, such as poly (methyl methacrylate) in *p*-xylene, polyimide in n-methyl-2-pyrrolidone, and polystyrene in toluene; unfortunately, we could not observe significant structural improvements of the P3HT films with these materials. The absorption spectra of these films are shown in Fig. S2.

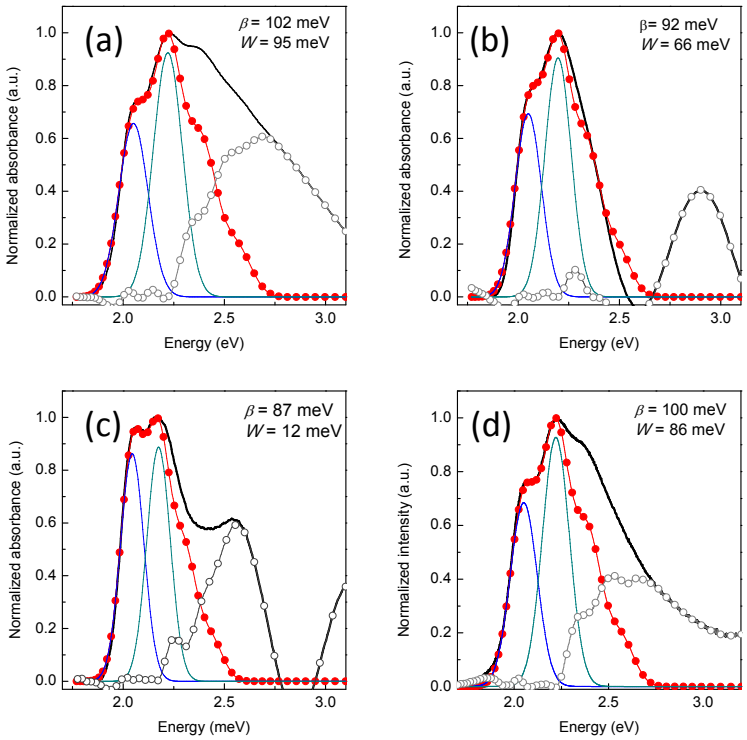

Fig. S1. Absorption spectra of various P3HT films: (a) the initial film; (b) after covering cPVP layer; (c) after covering LiF layer, then QSRC processing; (d) the post-annealed film (175 ^{o}C, 1 h). The solid lines represent the experimental data. The lines with closed symbols represent the theoretical fit obtained by using Eq. (S1), while the lines with open symbols represent the residual curve between the experimental and theoretical curves. Only the theoretical modelling of A_0 and A_1 bands are shown and these are plotted as thin lines. The exciton bandwidth (W) and the half width of individual vibronic bands (β) of the crystalline portions of the films are also shown.

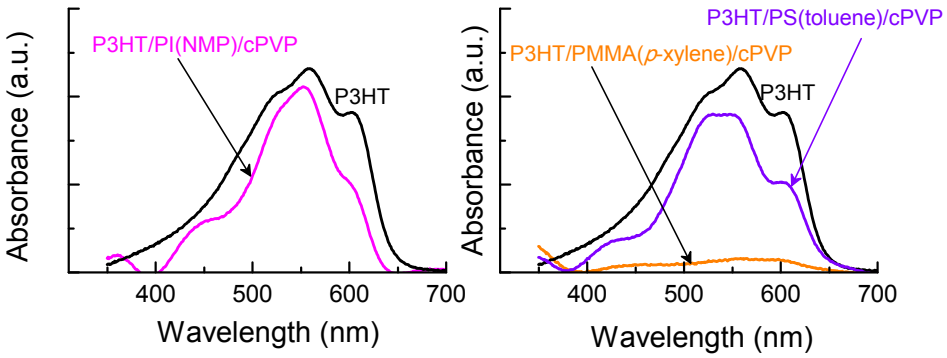

Fig. S2. Absorption spectra of the P3HT films with and without covering polymeric bilayer insulators. Note: PI(NMP): polyimide from n-methyl-2-pyrrolidone solution; PMMA(p-xylene): poly(methyl methacrylate) from *p*-xylene solution; PS(toluene): polystyrene from toluene solution.

3. Quantum chemical calculations details

The geometry of the thiophene monomer was first optimized using the DFT at B3LYP/6-31G(d) level of theory with periodic boundary conditions. The optimized geometry structure was then used to produce the polythiophene with different chain lengths and the corresponding parallel dimers with the interchain π-π stacking of 0.38 nm.[11] The J_{nm} of the dimers in various chain length were calculated using the ZINDO/S Hamiltonian and the results were shown in Fig. S3(A). The geometry of the polythiophene chains with different N at neutral and cationic states were first optimized using the DFT at B3LYP/6-31G(d) level of theory. The optimized structure was likewise used to calculate the λ_{reorg} described by other studies.[3,19b] The λ_{reorg} results were shown in Fig. S3(B). The vibrational frequency calculations of oligo(thiophene)s with thiophene units were performed by using DFT at the B3LYP/6-31G(d) level of theory. All the calculations were performed using the Gaussian suite of programs.[S1]

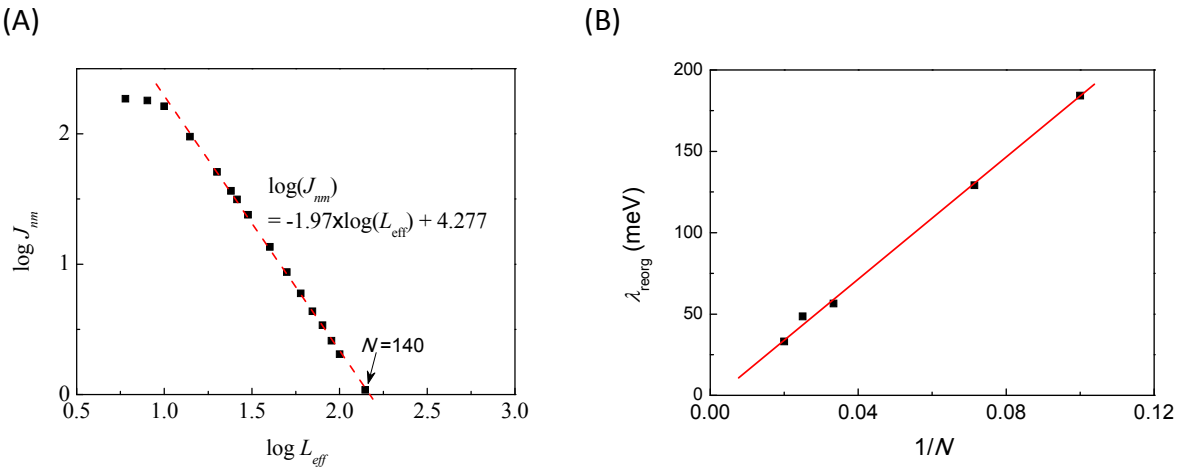

Fig. S3. (A) Double-logarithmic plots of J_{nm} versus L_{eff} of parallel polythiophene chains with separation distance of 0.38 nm. The dashed line was obtained by fitting the data with the first least square method. The L_{eff} was defined as the number of repeat units (N). (B) Plots of J_{nm} versus $1/N$ of polythiophene chains with different N. The line was obtained by fitting the data with the first least square method.

4. Application to FET devices

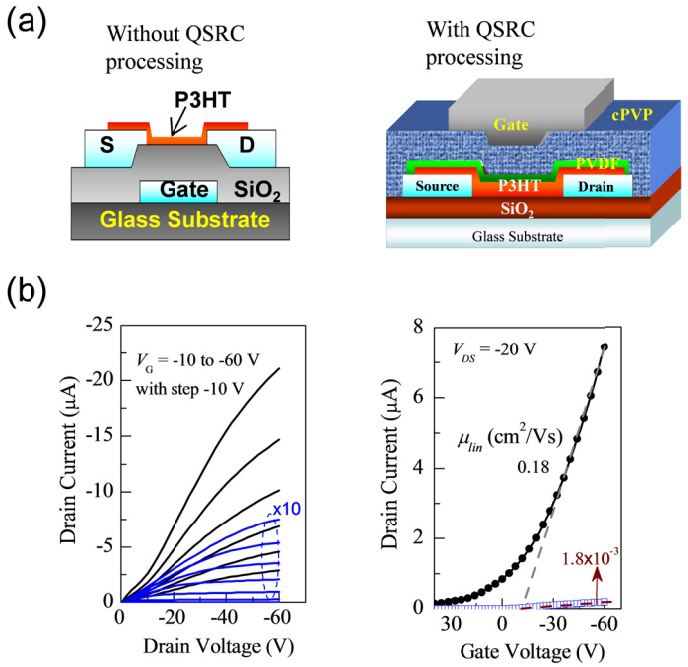

Fig. S4. (a) Schematic diagram of the FETs configuration. **Left panel**: A conventional bottom gate-bottom contact FET. The FET substrate with prefabricated indium-tin-oxide (ITO) as the gate and source/drain electrodes and a conventional silicon dioxide (SiO_2) as gate dielectric used in the experiments have been described previously.[S2] The dry film (ca. 60 nm) was prepared onto the active channel and referred as the A device. **Right panel**: a top-gate-bottom-contact FET with the PVDF/cPVP as the gate dielectric, ITO as source/drain electrodes, and Ag as the gate electrode. The QSRC-treated film (ca. 50 nm) was prepared onto the active channel and referred as the B device. (B) Comparison of output (left panel) and transfer (right panel) characteristics of the A (blue lines) and B (black lines) devices. The linear regime field-effect mobility (μ_{lin}) was extracted by the conventional transconductance method.

Note 1: The electrical characteristics of FET devices were measured by a Keithley 4200-SCS semiconductor parameter analyzer in a dark nitrogen-filled glove box. The capacitance of the dielectrics was measured using impedance spectroscopy (Agilent 4980A).

Note 2: The output curves of the B device show current crowding pheneomena at low drain voltages, thus indicating the non-ideal contacts between the ITO electrodes and P3HT active layer. This means that it's possible to further improve the performance of P3HT FETs by optimizing the fabrication conditions. Introducing the QSRC concept in developing high-performance polymeric optoelectronics is now in progress; the results will be published elsewhere and these topics is beyond the scope of the present paper.

References

S1 M. J. Frisch et al., *Gaussian 03, Revision E.01*, Gaussian, Inc., Wallingford , CT, 2004; *Gaussian 09, Revision A.02*, Gaussian, Inc., Wallingford , CT, 2009.

S2 H. L. Cheng, W. Y. Chou, C. W. Kuo, Y. W. Wang, Y. S. Mai, F. C. Tang and S. W. Chu, *Adv. Funct. Mater.,* 2008*,* **18**, 285.